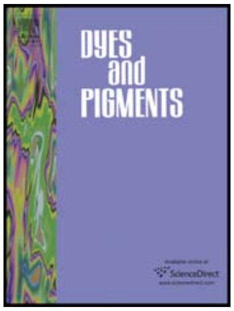

# Tuning the optoelectronic properties of cyanine and ketocyanine dyes by incorporation of 9,9-di-*n*-propylfluorenylindolenine

R.D. Jansen-van Vuuren, P.C. Deakin, S. Olsen, P.L. Burn

PII: S0143-7208(13)00328-8
DOI: 10.1016/j.dyepig.2013.09.003
Reference: DYPI 4077

To appear in: *Dyes and Pigments*

Received Date: 16 August 2013

Accepted Date: 4 September 2013

Please cite this article as: Jansen-van Vuuren RD, Deakin PC, Olsen S, Burn PL, Tuning the optoelectronic properties of cyanine and ketocyanine dyes by incorporation of 9,9-di-*n*-propylfluorenylindolenine, *Dyes and Pigments* (2013), doi: 10.1016/j.dyepig.2013.09.003.

## Graphical abstract

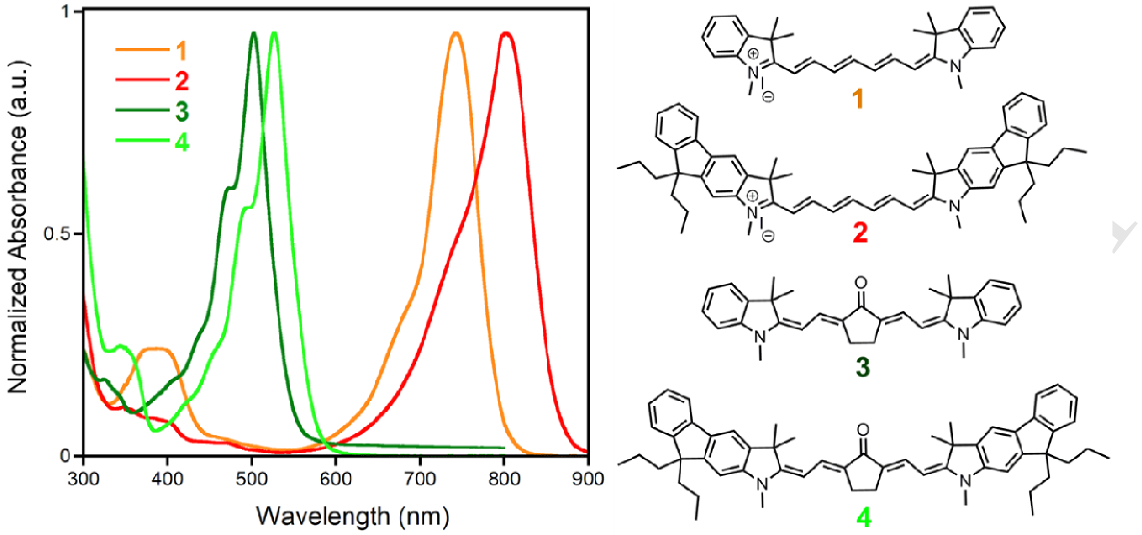

# Tuning the optoelectronic properties of cyanine and ketocyanine dyes by incorporation of 9,9-di-*n*-propylfluorenylindolenine

Author names and affiliations: R. D. Jansen-van Vuuren,[a] P. C. Deakin,[b] S. Olsen,[a,c] P. L. Burn[a,b]

[a]Centre for Organic Photonics & Electronics (COPE), The University of Queensland, 4072 Queensland, Australia
[b]Department of Chemistry, Chemistry Research Laboratory, University of Oxford, Mansfield Rd, OX1 3TA Oxford, United Kingdom
[c]School of Mathematics & Physics, The University of Queensland, 4072 Queensland Australia

[b]Corresponding author. Tel: +61 7 3346 7614
Email addresses: p.burn2@uq.edu.au (P. L. Burn)

## Abstract:

The synthesis and properties of novel cyanine and ketocyanine dyes incorporating 9,9-di-*n*-propylfluorenyl units is reported. While bathochromic shifts of order 100 nm are observed in (keto)cyanines for addition of each vinylene unit (lengthening the methine chain) it was observed that addition of the fluorenyl unit enabled fine tuning of the UV-visible absorption spectrum. The hypsochromic shift in the UV-visible absorption spectrum of the ketocyanines relative to the corresponding cyanine dyes was found to be consistent with the Dewar-Knott colour rule. The oxidation ('Highest Occupied Molecular Orbital energy') and reduction ('Lowest Unoccupied Molecular Orbital energy) potentials were also qualitatively consistent with the Dewar-Knott colour rule, with the 'HOMO energies' of the comparative dyes being the same and the LUMO energies of the ketocyanines being destabilised relative to the cyanine dyes.

**Keywords:** Cyanine, Ketocyanine, Organic Semiconductor, Fluorenyl, Photodiodes, Solar Cells

## Highlights

- Cyanine and ketocyanine dyes have been synthesized incorporating a fluorenyl unit within the indolenine end-group.
- Inclusion of the 9,9-di-*n*-propylfluorenyl units enables fine-tuning of the optoelectronic properties of cyanine and ketocyanine dyes.

- The absorption properties of the dyes follow the Dewar-Knott colour rule with the electrochemical properties of the materials experimentally confirming the theory.

## 1. Introduction

The development of organic semiconductors has experienced remarkable progress over the past decade [1] as their use in a range of applications including photovoltaic (PV) cells [2,3], light-emitting diodes [4], thin-film transistors [5,6], and organic photodetector (OPD) arrays for image sensing [7-11] has been realized. Organic semiconductors offer many potential benefits for these applications including the prospect of simple processing methods (*e.g.*, solution deposition), the possibility of lightweight, thin, and flexible devices, and the existence of a wide selection of organic materials, which allows for tuning of the physical and optoelectronic properties [12,13].

Recent reports have highlighted the incorporation of organic dyes in small molecule organic PV (OPV) [14-16] and OPD devices [10,17,18] due to their strong light absorption and good solution processability. One class of dye that has received attention with respect to OPVs are the cyanines, a group of charged polymethine dyes [19-22]. A strong emphasis of current OPV research has been on the development narrow optical gap materials, often called 'low band-gap' materials, that are designed to absorb as much of the solar spectrum as possible [23,24]. The creation of cyanine dyes with a narrow optical gap is therefore a core objective for organic PV applications, with a particular focus on materials that absorb in the Near-Infrared (NIR) [25,26]. The long-wavelength absorption peak of cyanines is typically controlled through the number of methine linkages, with a red shift in the peak wavelength of ~100 nm per additional methine group generally observed.[21] However, the stability of cyanine dyes decreases with an increase in the polymethine length [27], with the methine bridges being susceptible to oxidation.

Ketocyanines are the neutral cyanine equivalents, which have been studied as the light absorbing materials in OPDs for visible image-sensing applications [11]. The advantage of having a non-charged dye is that counterion migration, which can degrade device performance [21,28], is avoided. Counterion migration is a significant issue for OPDs, which are typically operated under a reverse (negative) bias [29]. An interesting feature of the ketocyanine dyes is that they generally have a narrow full-width-half-maximum, which is important to achieve spectrally selective colour sensors [30, 31]. However, a second requirement for spectrally selective colour sensors is that the absorption maximum of each sensor needs to be at different and specific wavelengths [32]. As in the case of the cyanine dyes, the wavelength selectivity can also be achieved at a coarse level by increasing the number of methine units although the same issues of stability arise as the number of double bonds increases.

An alternative strategy for tuning the absorption of cyanine and ketocyanine dyes is to extend the conjugation of the indolenyl moiety of the dyes. Thus, in this manuscript we describe the synthesis and optoelectronic properties of fluorenylindolenine cyanine **2** and fluorenylindolenyl ketocyanine **4** and compare them with their parent cyanine and ketocyanine dyes, **1** and **3**, respectively (Figure 1). A further advantage of the 'fluorenyl moiety' is that the *n*-propyl chains attached to the bridgehead benzyl-position improve the solubility of the dyes. Finally, while the structure-property relationships of cyanine dyes have been studied [33], this work will impart valuable information for predicting the properties of the less well-known ketocyanines.

## 2. Experimental

### 2.1. General information

Unless otherwise noted, all chemicals were obtained from commercial suppliers (Sigma Aldrich, Alfa Aesar, Unilab) and used as received. Molecular sieves (3Å and 4Å) were activated for use by heating at 250 °C under reduced pressure ($10^{-1}$-$10^{-2}$ mbar) for 24 h. All solvents were distilled prior to use. Acetonitrile was dried over anhydrous potassium carbonate for 24 h, dried over 3Å molecular sieves for 24 h before distilling onto and storing over 4Å molecular sieves. Pyridine was dried by refluxing over calcium hydride for 30 min followed by fractional distillation onto activated 4Å molecular sieves. Tetrahydrofuran was freshly distilled over sodium benzophenone ketal. Column chromatography was performed with Kieselgel 60 230-400 mesh silica purchased from Merck (cat. number 1.09385.9025). Materials that were purified with >5% methanol in chloroform mixtures were further dissolved in the minimum dichloromethane and passed through a plug of Celite to remove any dissolved silica gel. Thin layer chromatography (TLC) was performed on aluminium plates coated with silica gel 60 F254. $^{1}$H and $^{13}$C NMR spectroscopy was performed on Bruker Avance AV-300, AV-400 or AV-500 MHz spectrometers: AR H = aryl H; IND H = indolenyl H; VIN H = vinyl H; br = broad; CP H = cyclopentanone H; FL H = fluorenyl H; PR H = *n*-propyl H. Coupling constants are given to the nearest 0.5 Hz. UV-visible spectroscopy was performed on a Cary 5000 UV-Vis spectrophotometer as a solution in spectroscopic grade solvent: sh = shoulder. FT-IR spectroscopy was performed on solid samples using a Perkin-Elmer Spectrum 100 FT-IR Spectrometer with an ATR attachment. Melting points ($T_m$s) were measured in a glass capillary on a Buchi B-545 melting point apparatus and are uncorrected. Microanalyses were carried out on a Carlo Erba NA 1500 Elemental Analyser. Matrix-assisted laser-desorption ionisation time of flight (MALDI-ToF) mass spectrometry were carried out on a Voyager DE STR MALDI-ToF spectrometer from dithranol (as matrix) in positive reflectron mode. Electrospray ionisation mass spectrometry was performed on a BRUKER HCT 3D Ion Trap mass spectrometer. Glass transition temperatures ($T_g$) were determined using a Perkin-Elmer Diamond Differential

Scanning Calorimeter. Thermal stability was determined by Thermal Gravimetric Analysis (TGA) under a nitrogen atmosphere using a Perkin-Elmer STA 6000 Simultaneous Thermal Analyser. Thermal decomposition values were reported as the temperature corresponding to a 5% sample mass reduction [$T_{d(5\%)}$].

### 2.2. Electrochemical Measurements

Electrochemistry was performed on an Epsilon Basi C3 Cell Stand with a glassy carbon working electrode, platinum counter electrode and silver reference electrode in 0.01 M silver nitrate in acetonitrile. Cyanines: oxidations and reductions were measured in fresh dry-distilled acetonitrile. Samples (1 mM) were dissolved with 0.1 M tetra-*n*-butylammonium tetrafluoroborate as the supporting electrolyte and degassed for 15 min with argon immediately prior to the electrochemical measurements. Ketocyanines: Oxidations were measured in freshly distilled dry dichloromethane [distilled over calcium hydride (5% w/v) under nitrogen] and reductions were measured in freshly double distilled dry tetrahydrofuran (first distilled over sodium/benzophenone, then from lithium aluminium hydride). Samples (1 mM) were dissolved with electrochemical grade tetra-*n*-butylammonium perchlorate (0.1 M) (Alfa Aesar cat. number 043999) as the supporting electrolyte, and degassed for 15 min with argon immediately prior to the electrochemical measurements. $E_{½}$ values are reported relative to the ferrocenium/ferrocene standard [34] which was measured on the same day using the same solvent and measurement conditions as the respective samples. Where the cyclic voltammetry showed that the redox processes were chemically reversible but lacked a clearly defined $E_{pa}$ or $E_{pc}$, Differential Pulse Voltammetry (DPV) was used to determine the $E_{1/2}$.

### 2.3. Organic Synthesis

#### 2.3.1. 1,1',3,3,3',3'-Hexamethylindotricarbocyanine iodide (**1**)

Triethylamine (190 μL, 1.36 mmol) was added to a mixture of 1,2,3,3-tetramethyl-3*H*-indolium iodide (211 mg, 0.70 mmol), *N*-(5-anilino-2,4-pentadienylidene)aniline hydrochloride (100 mg, 0.35 mmol) and acetic anhydride (130 μL, 1.38 mmol) in methanol (10 mL), and the resultant mixture deoxygenated by three vacuum-nitrogen purging cycles. The reaction was then stirred at room temperature in the dark for 16.5 h followed by removal of the volatiles *in vacuo*. The crude material was taken up in the minimum amount of dichloromethane (<10 mL) and precipitated into ether (200 mL). The precipitate was isolated by centrifugation (3 min at 3000 rpm) followed by decantation of the supernatant and drying. The precipitate was collected and further purified by column chromatography over silica using methanol/chloroform (1:9) as eluent followed by removal of the solvents and recrystallization from an ethanol/petroleum mixture to give **1** as a green crystalline solid (77 mg, 41%), which had an identical $^1$H NMR spectrum and ES-MS as the literature [35].

### 2.3.2. Di-*tert*-butyl-1-(9,9-di-*n*-propyl-9*H*-fluoren-2-yl)hydrazine-1,2-dicarboxylate (**6**)

*n*-Butyllithium (1.6 M, 6.4 mL, 10 mmol) was added slowly to a stirred solution of 9,9-di-*n*-propyl-2-bromofluorene, **8** (2.8 g, 8.5 mmol) in tetrahydrofuran (50 mL) at -78 °C, under nitrogen. After stirring for 30 mins, di-*tert*-butylazodicarboxylate (4.31g, 18.6 mmol) dissolved in tetrahydrofuran (50 mL) was added to the reaction mixture. After stirring at -78 °C for 2 h, the mixture was allowed to warm to room temperature and stirred for a further 18 h. Glacial acetic acid (1.81 mL) was added slowly and the mixture stirred for a further 4 h at room temperature. Ether (50 mL) and water (50 mL) were added. The aqueous layer was separated and extracted with ether (2 x 60 mL). The combined organic extracts were then washed with brine (60 mL), dried over magnesium sulphate, filtered and the solvent completely removed. The crude material was purified by column chromatography over silica using dichloromethane as eluent to give **6** as a white amorphous powder (2.42 g, 64%); $T_{d(5\%)}$ 220 °C; $T_g$ 50 °C; (Found C, 72.35%; H, 8.35%; N, 5.9%. $C_{29}H_{40}N_2O_4$ requires C, 72.5%; H, 8.4%; N, 5.8%); $\nu_{max}$ (solid)/cm$^{-1}$ 1705 (C=O); $\lambda_{max}$ (THF) 247 nm sh (log ε/dm$^3$ mol$^{-1}$ cm$^{-1}$ 3.57), 253sh (3.75), 281(4.28), 289sh (4.24) , 306 (4.13), 313sh (4.05); $\delta_H$ (400.1 MHz, $CDCl_3$) 0.65 (10 H, brm, PR $CH_2$ & $CH_3$), 1.50 (18 H, brs, 2 x *tert*-Bu), 1.92-1.98 (4 H, brm, PR $CH_2$), 6.63 and 6.84 (tautomers) (1 H, br s, N-H/O-H), 7.26-7.44 (5 H, m, FL H), 7.61-7.68 (2 H, m, FL H); $\delta_C$ (100.6 MHz, $CDCl_3$) 14.4, 17.1, 28.0, 28.15, 28.17, 42.7, 55.3, 81.5 (br), 82.1, 119.4, 119.5, 122.8, 126.7, 126.8, 138.7 (br), 140.5, 141.4 (br), 150.9 (br), 153.8 (br), 155.4 (br) (the doubling up of peaks is due to the different tautomers); *m/z* [ESI: 5% DCM, MeOH] found 479.4 (100%), 480.3 (32%), 481.3 (6%), 482.2 (1%); $C_{29}H_{40}N_2O_4$ requires 480.30 (100%), 481.30 (32%), 482.30 (1%), 482.31 (5%).

### 2.3.3. 2-(9,9-Di-*n*-propyl-9*H*-fluoren-2-yl)hydrazin-1-ium chloride (**7**)

A solution of concentrated hydrochloric acid (4.1 mL) in 1,4-dioxane (12.5 mL) was added to a solution of **9** (2.0 g, 4.1 mmol) in 2-propanol (22.7 mL). The reaction mixture was heated at 85 °C for 1 h. After cooling to room temperature, the solvent was completely removed to give **7** as a pink amorphous solid (1.2 g, 95%); mp 172-175 °C; (Found C, 72.0%; H, 8.1%; N, 8.6%. $C_{19}H_{25}ClN_2$ requires C, 72.0%; H, 7.95%; N, 8.8%); $\nu_{max}$ (solid)/cm$^{-1}$ 3324 (NH), 3220-2500 (NH and CH); $\lambda_{max}$ (EtOH) 306sh nm (log ε/dm$^3$ mol$^{-1}$ cm$^{-1}$ 4.30), 316 (4.35), 336sh (4.28), 349sh (4.01); $\delta_H$ (400.1 MHz, DMSO-$d_6$) 0.48-0.65 (10 H, m, PR $CH_2$ & $CH_3$), 1.81-1.97 (4 H, m, PR $CH_2$), 6.91 (1 H, dd, $J$ = 8 Hz, $J$ = 2 Hz, FL H), 7.04 (1 H, d, $J$ = 2 Hz, FL H), 7.20-7.28 (2 H, m, FL H), 7.37 (1 H, d, $J$ = 8 Hz, FL H), 7.66-7.70 (2 H, m, FL H), 8.28 (1 H, br s, NH), 10.14 (3 H, br s, $NH_3^+$); $\delta_C$ (100.6 MHz, DMSO-$d_6$) 14.2, 16.9, 42.0, 54.8, 109.3, 113.4, 119.1, 120.3, 122.8, 126.3, 126.9, 134.5, 140.4, 145.1, 149.6, 151.5; *m/z* [ESI: 5% DCM, MeOH] found: 281.1 (100%), 282.1 (34%); $C_{19}H_{25}N_2^+$ requires 281.2 (100%), 282.2 (21%), 283.2 (2%).

### 2.3.4. 2,3,3-Trimethyl-9,9-di-*n*-propyl-3,9-dihydroindeno[1,2-f]indole (**8**)

Concentrated sulphuric acid (1.4 mL) was added dropwise to a mixture of **7** (1.22 g, 3.86 mmol) and 3-methylbutan-2-one (1.25 mL, 11.6 mmol) in ethanol (28 mL). The reaction mixture was heated at 85 °C for 48 h. After cooling, the solvent was removed and the residue was taken up in diethyl ether (50 mL). The organic layer was washed with aqueous potassium hydroxide (5% w/v, 50 mL), and the aqueous layer was extracted with diethyl ether (2 x 50 mL). The combined organic extracts were dried over magnesium sulphate, filtered and the solvent removed. The residue was purified by column chromatography over silica using dichloromethane as eluent to give **8** as a viscous yellow oil (721 mg, 56%); (Found C, 86.7%; H, 8.8%; N, 4.3%. $C_{24}H_{29}N$ requires C, 87.0; H, 8.8; N, 4.2); $\lambda_{max}$ (THF) 224sh nm (log $\varepsilon$/dm$^3$ mol$^{-1}$ cm$^{-1}$ 4.36), 235 (4.18), 243 (4.15), 253sh (4.04), 259sh (4.12), 291 (4.40), 299 (4.39), 311 (4.34), 318 (4.26), 325 (4.32); $\delta_H$ (400.1 MHz, $CDCl_3$) 0.63-0.70 (10 H, m, PR $CH_2$ & $CH_3$), 1.37 (6 H, s, $C(CH_3)_2$), 1.93-2.00 (4 H, m, PR $CH_2$), 2.30 (3 H, s, $CH_3$), 7.24-7.34 (3 H, m, FL H), 7.48 (1 H, brs, FL H), 7.57 (1 H, d, *J* = 0.5 Hz, FL H), 7.66 (1 H, m, FL H); $\delta_C$ (100.6 MHz, $CDCl_3$) 14.4, 15.5, 17.1, 23.4, 42.8, 53.2, 55.0, 112.5, 114.5, 119.1, 122.8, 126.4, 126.6, 138.3, 141.1, 144.8, 150.9, 151.1, 153.5, 187.9; *m/z* [ESI: 5% DCM, MeOH] found 332.2 (100%), 333.2 (26%), 334.2 (5%); $C_{24}H_{29}N$ requires 331.2 (100%), 332.2 (26%), 333.2 (3%).

### 2.3.5. 1,2,3,3-Tetramethyl-9,9-di-*n*-propyl-3,9-dihydroindeno[1,2-f]indol-1-ium iodide (**9**)

A mixture of **8** (111 mg, 0.34 mmol) and iodomethane (0.25 mL, 4.02 mmol) in acetonitrile (5 mL) was heated under nitrogen at 85 °C for 22 h. The reaction mixture was cooled to room temperature before the solvent and excess iodomethane were completely removed *in vacuo*. The residue was sonicated with diethyl ether (15 mL) for 5 min before the solvent was decanted and the residual solid dried to give **9** as a yellow/green amorphous powder (150 mg, 95%); mp 235-237 °C; (Found C, 63.2%; H, 6.8%; N, 2.95%. $C_{25}H_{32}IN$ requires C, 63.4%; H, 6.8%; N, 3.0%); $\lambda_{max}$ (THF) 225sh nm (log $\varepsilon$/dm$^3$ mol$^{-1}$ cm$^{-1}$ 4.14), 237 (3.95), 253sh (3.74), 261 (3.72), 268sh (3.75), 298sh (3.93), 320 (4.29), 337 (4.28), 382sh (3.59); $\delta_H$ (300.1 MHz, $CDCl_3$) 0.60-0.73 (10 H, m, PR $CH_2$ & $CH_3$), 1.72 (6 H, s, $C(CH_3)_2$), 1.99-2.07 (4 H, m, PR $CH_2$), 3.19 (3 H, s, $CH_3$), 4.39 (3 H, s, $NCH_3$), 7.38-7.41 (3 H, m, FL H), 7.56 (1 H, brs, FL H), 7.73-7.77 (1 H, m, FL H), 7.79 (1 H, brs, FL H); $\delta_C$ (100.6 MHz, $CDCl_3$) 14.3, 17.1, 17.3, 23.3, 37.4, 42.5, 54.1, 56.0, 109.7, 114.0, 120.4, 127.3, 128.7, 138.7, 140.9, 143.7, 151.4, 153.1, 194.8; *m/z* [ESI: MALDI ToF: DITH] found 346.2 (100%), 347.2 (61%), 348.2 (11%). $C_{25}H_{32}N^+$ requires 346.2 (100%), 347.3 (27%), 348.3 (4%).

### 2.3.6. 1,3,3-Trimethyl-9,9-di-*n*-propyl-2-[(1*E*,3*E*,5*E*,7*E*)-7-(1,3,3-trimethyl-9,9-di-*n*-propyl indeno[1,2-f]indol-2{1*H*,3*H*,9*H*}-ylidene)hepta-1,3,5-trien-1-yl]-3,9-dihydroindeno[1,2-f]indol-1-ium iodide (**2**)

Triethylamine (90 μL) was added to a stirred solution of **9** (150 mg, 0.32 mmol), *N*-[5-(phenylamino)-2,4-pentadienylidene]aniline monohydrochloride (45 mg, 0.2 mmol) and acetic anhydride (0.90 mL, 9.5 mmol) in methanol (4.5 mL). The reaction mixture was deoxygenated by three vacuum-nitrogen purging cycles, and left to react at room temperature for 23 h under nitrogen, before the solvent was removed. The crude product was precipitated by dissolving in dichloromethane (8 mL) and adding this solution to diethyl ether (60 mL), before centrifuging the suspension at 3000 rpm for 15 min. The supernatant was decanted and the residue dried to give **2** (48 mg, 34%) as a copper-orange coloured solid; $T_{d(5\%)}$ 233 °C; UV-vis (THF): $\lambda_{max}$ (THF) 280 nm (log $\varepsilon/dm^3\ mol^{-1}\ cm^{-1}$ 4.81), 366 (4.06), 402 (3.97), 416 sh (3.78), 475sh (3.54), 736sh (4.74), 803 (5.07); $\delta_H$ (400.1 MHz, $CDCl_3$) 0.60-0.70 (20 H, m, PR $CH_2$ & $CH_3$), 1.74 (12 H, brs, $C(CH_3)_2$), 1.91-2.03 (8 H, m, PR $CH_2$), 3.73 (6 H, brs, N-$CH_3$), 6.28 (2 H, br d, VIN H), 6.68 (2 H, br m, VIN H), 7.02 (2 H, s, FL H), 7.27-7.36 (6 H, m, FL H), 7.60 (2 H, s, FL H), 7.65-7.68 (2 H, m, FL H), 7.80 (3 H, br m, VIN H); *m/z* [ESI: 5% DCM, MeOH] found: 753.5 (100 %), 754.5 (58%), 755.5 (17%), 756.5 (4%). $C_{55}H_{66}N_2^+$ requires 753.5 (100%), 754.5 (60%), 755.5 (18%), 756.5 (4%).

### 2.3.7. (2*E*,5*E*)-2,5-Bis[(*E*)-2-(1,3,3-trimethyl-9,9-di-*n*-propylindeno[1,2-f]indol-2-{1*H*,3*H*,9*H*}-ylidene)ethylidene]cyclopentanone (**4**)

A solution of **9** (102 mg, 0.22 mmol) and enaminocyclopentanone **10** (21 mg, 0.1 mmol) in pyridine (2.1 mL) was heated at reflux for 1.5 h. The reaction mixture was then allowed to cool to room temperature before being diluted with water (40 mL), filtered and the residue dried *in vacuo*. The crude product was purified using column chromatography over silica using hexane:ethyl acetate mixtures (1:0 to 1:4 to 2:3) as eluent to give **4** as a purple/gold solid (107 mg, 25%); $T_{d(5\%)}$ 330 °C; $T_g$ 145 °C; $\nu_{max}$ (solid)/$cm^{-1}$ 1567 (C=O); $\lambda_{max}$ (THF) 277 nm (log $\varepsilon/dm^3\ mol^{-1}\ cm^{-1}$ 5.15), 346br (4.50), 420sh (4.17), 454sh (4.47), 492 (4.85), 527 (5.08); $\delta_H$ (300.1 MHz, toluene-$d_8$) 0.61-0.85 (20 H, m, PR $CH_2$ & $CH_3$), 1.67 (12 H, s, $C(CH_3)_2$), 1.85-2.00 (8 H, m, PR $CH_2$), 2.66 (6 H, s, N-$CH_3$), 2.79 (4 H, m, CP H), 5.34 (2 H, d, *J* = 13 Hz, VIN H), 6.50 (2 H, s, FL H), 7.18-7.53 (10 H, m, FL H), 8.23 (2 H, d, *J* = 13 Hz, VIN H); *m/z* [ESI: 5% DCM, MeOH] found: 795.6 (100.0%), 796.6 (60.5%), 797.6 (21.0%) ($MH^+$). $C_{57}H_{66}N_2O$ requires 794.5 (100.0%), 795.5 (62.4%), 796.5 (19.3%), 797.5 (4.0%).

## 3. Results and Discussion

### 3.1. Synthesis

Indotricarbocyanine **1** was synthesised in a 41% yield using a procedure that has been successfully used for shorter cyanine dyes [36] (Scheme 1). The synthetic route to ketocyanine dye **3** has previously been reported [37]. The strategy used to obtain fluorenylcyanine **2** and fluorenylketocyanine dye **4** is shown in Scheme 2, with the salt **9** the common intermediate. Transmetallation of 2-bromo-9,9-di-*n*-propylfluorene **5** with *n*-butyllithium, and subsequent reaction of the anion formed with di-*t*-butylazodicarboxylate (DBAD) provided the *N*-*t*-butoxycarbonyl (*t*-BOC)-protected hydrazine **6** in a 64% yield. Deprotection *via* acid hydrolysis resulted in the formation of the hydrazine hydrochloride **7** in a yield of 95%. The Fischer-Indole method [38] facilitated the ring-closure and formation of fluorenylindolenine **8** (56% yield), which was subsequently methylated to form the iodide salt **9** in a 95% yield. To form the fluorenylcyanine **2** the iodide salt **9** was reacted with *N*-[5-(phenylamino)-2,4-pentadienylidene]aniline monohydrochloride whereas to form **4**, **9** was reacted with enaminocyclopentanone **10**. **2** was purified by precipitation and isolated in a 34% yield, whilst chromatography over silica resulted in the isolation of **4** in a 25% yield. It is important to note that the $^1$H n.m.r. spectrum of **4** was more complicated than expected for the all *trans* product. The complexity of the $^1$H n.m.r. spectrum was similar to that observed for the parent chromophore **2**, with the extra signals arising from different geometric isomers [11]. In addition, small signals were sometimes observed in the aldehydic region, indicating that care had to be taken to avoid hydrolysis of the ketocyanines.

### 3.2. Properties of the materials

The first stage in the analysis of the materials was determination of their thermal properties by Differential Scanning Calorimetry (DSC) and Thermal Gravimetric Analysis (TGA). TGA was undertaken at a scan rate of 50 °C/min under nitrogen and the decomposition temperature was taken as the temperature corresponding to a 5% weight loss [$T_{d(5\%)}$]. The ketocyanines were found to be more stable than the cyanines with decomposition temperatures approximately 100 °C higher [**1** (203 °C) and **2** (233 °C) *versus* **3** (345 °C) and **4** (330 °C)]. The greater stability of the ketocyanine is directly related to the presence of the cyclopentanone unit rather than the conjugated vinylene units in the cyanines. It is interesting to note that the extension of the indolenyl unit did not change the thermal stability significantly. DSC analysis (scan rate 100 °C/min) showed that only **4** had a $T_g$ (145 °C), which was more than 100 °C below the melting point of the parent dye **3**.

We next investigated the optical properties of the materials with the solution (tetrahydrofuran) absorption spectra of **1**-**4** shown in Figure 2. The short wavelength features at around 350 nm for the dyes are due to π-π* transitions of the arylindolenyl unit (a fluorenyl unit absorbs at 250-320 nm [39]). The strong longer wavelength absorptions observed for both sets of compounds are reported to be associated with a donor-acceptor Intramolecular Charge Transfer (ICT) transition that occurs over the polymethine-bridge. For **1** and **2** (the cyanines), the donor and acceptor refer to the two nitrogen centres: for each resonance contributor, one of these will be positively charged, therefore acting as the acceptor, whilst the other nitrogen is the donor, and a ‘push-pull’ feature enables the ICT to occur [33]. In the case of the ketocyanines **3** and **4**, the ICT takes place from the amine donor to carbonyl acceptor, and the shoulder observed at 480-490 nm is due to interaction of the two chromophores within the bichromophoric system [40]. For the long wavelength ICT absorptions in moving from indolenyl to the fluorenylindolenine, the Full Width at Half Maximum (FWHM) increases for the cyanine dyes by ~30 nm, from 66 nm for **1** to around 95 nm for **2**, while for the ketocyanines dyes **3** and **4** the FWHM is essentially the same at 64-65 nm. It is important to note that these FWHM are sufficient to enable imaging with colour constancy in photodiode applications [32].

However, in both series in moving from the indolenyl to the fluorenylindolenine moiety, there is a red shift in the absorption maxima – from 743 nm to 802 nm for **1** and **2**, and 502 nm to 527 nm for **3** and **4**. The red shift between cyanines **1** and **2** and the ketocyanines **3** and **4** caused by the introduction of the fluorenyl 'end group' is the same at 0.12 eV. The addition of an extra vinyl moiety within the cyanine chromophore changes the absorption maxima bathochromically by approximately 100 nm [41, 42], that is, for a parent dye absorbing at 743 nm, an additional vinyl unit would be expected to reduce the optical gap by 0.2 eV. The observed red shift by the addition of the fluorenyl 'end group' is significantly smaller than expected for an equivalent physical extension of the charge conjugation path of the parent cyanine chromophore, and hence the results show that modification of the indolenyl unit enables fine-tuning of the absorption wavelength. In contrast, there is a large difference between the cyanine and ketocyanine chromophores that have nominally the same number of methine carbons between the two nitrogen atoms (most easily seen when the ketocyanine is drawn in the enolate form with a positive charge on one of the nitrogens). Comparing the change in the optical absorption wavelength in energy units (eV) between the cyanine **1** ($\lambda_{max}$ = 1.67 eV) and the ketocyanine **3** ($\lambda_{max}$ = 2.47 eV) yields a shift of 0.80 eV that can be attributed to the influence of the oxy substituent upon the excitation energy of the underlying cyanine **1**. The same shift was also observed between cyanine **2** ($\lambda_{max}$ = 1.55 eV) and ketocyanine **4** ($\lambda_{max}$ = 2.35 eV). These observations indicate that the effect of the oxy substituent in the middle of the methine chain (termed the *meso*-position in the chain) and the fluorenylindole end-groups are each affecting local, independent and additive changes in the spectra of the dyes studied. The hypsochromic shift observed between dyes **1** and **3** (equivalently, between **2** and **4**) is close to the range of energy shifts that are observed in chemically similar cases. For example, it is somewhat smaller than the shift obtained upon comparison of Michler's Hydrol Blue [$\lambda_{max}$ = 615 nm (2.02 eV) in glacial acetic acid [43] with Michler's Ketone [$\lambda_{max}$ = 372 nm (3.33 eV) in the same solvent [44], and is similar in size to the shift between Michler's Hydrol Blue and Auramine-O [$\lambda_{max}$ = 441 nm (2.81 eV), also in glacial acetic acid [44]. The observation of a hypsochromic shift upon substitution at the *meso*-position in the chain with a strongly electron donating oxy-substituent is consistent with the Dewar-Knott colour rule [45, 46]. The Dewar-Knott colour rule is based on the structure of the Hückel orbitals of an odd-alternate hydrocarbon reference species [45] (the cyanine and ketocyanines of this work have five 'double bonds'). The rule has recently been shown to also be consistent with more modern electronic structure calculations for a series of dyes similar to those studied here [47]. In this analysis, the highest occupied orbital (HOMO) of the reference has a node at the *meso*-position, while the lowest unoccupied orbital (LUMO) does not. Substitution at the meso-position in the chain with electro-donating groups therefore destabilizes the LUMO while leaving the HOMO energy unchanged. If the electronic excitation is modelled as a one-electron excitation between these levels, this leads to the prediction of a blue shift, which is observed experimentally in this work. Thus, for the UV-visible absorption spectra of the dyes it can be concluded that the extension of the heterocyclic end-groups to include a fluorenyl moiety leads to a bathochromic shift that is the same for both cyanine and ketocyanine cases studied. The magnitude of this shift is significantly smaller than the bathochromic shift that is often observed in cyanines upon the lengthening of the polymethine chain (around 100 nm per vinylene unit [41, 42]). This argues against the interpretation of the bathochromic shift arising from the fluorenyl 'end groups' being due to the extension of the effective conjugation length of the polymethine. Instead, the shift can be explained by relative stabilization of the resonating charge at the chain termini (the iminium cation) by interaction with the polarizable fluorenyl $\pi$-electron system. A similar mechanism has been invoked by Spasokukotskii *et al.* to explain bathochromic shifts of similar size for cyanines containing indolyl, benzoxazolyl and thiazolyl end-groups [48].

In a final aspect of the analysis, the redox properties of the materials were studied by cyclic voltammetry (CV) and, where necessary, Differential Pulse Voltametry (DPV) in solution. Both reduction and oxidation measurements for **1** and **2** were carried out in acetonitrile and, in both cases, referenced against the ferrocenium/ferrocene couple. In all cases, four scans were carried out and no reduction in the current was observed, indicating that the redox processes were chemically reversible. The cyclic voltammograms for the oxidative processes of **1** and **2** are shown in Figure 3. The $E_{1/2}$s for the first oxidation of **1** and **2** were resolved with DPV and found to be -0.2 V for **1** and 0.0 V for **2**. The oxidation of the iodide counteranion has been previously reported to occur at around 0.4 V [49] and is therefore masked by the oxidative processes of the dyes. The $E_{1/2}$s for the first reduction of **1** and **2** were also resolved with DPV and found to be at -1.1 V for **1** and -1.0 V for **2**. The $E_{1/2}$s for the first oxidation and reductions of **3** and **4** were 0.0 V and -0.1 V (oxidations) and -2.2 V and -1.3 V (reductions), respectively (see Figure 4). Thus the electrochemical results qualitatively support the Dewar-Knott rule in that the oxidation potentials ('HOMO energy levels') are essentially the same for the cyanine and ketocyanine dyes while the 'LUMO energy' is destabilised (reductions at more negative potentials) for the ketocyanine dyes relative to the cyanine chromophores. That the electrochemical data are consistent with the Dewar-Knott rule in this way is a significant result. It suggests that the electrochemical and photophysical processes can be described by a common compact set of frontier orbitals. There is no obvious *a priori* reason to expect this because the photophysical process is electron number conserving while the electrochemical process is not.

## 4. Conclusion

Cyanine and ketocyanine dyes incorporating 9,9-di-*n*-propylfluorenyl units into end groups of the chromophores have been synthesized. The thermal, optical and electrochemical properties were investigated experimentally and compared with the parent chromophores. It was found that inclusion of the fluorenyl unit only had a small influence on the thermal properties of the dyes but led to a red shift in the absorption spectra compared with the parent dyes, thus enabling fine-tuning of the optical properties. The origin of the shift was understood to arise from stabilization of the resonating charge at the chain termini by interaction with the polarizable fluorenyl $\pi$-electron system. However, the largest difference in the absorption spectrum was observed between the equivalent cyanine and ketocyanine chromophores with the latter showing a strong hypsochromic shift. The hypsochromic shift could be explained by the Dewar-Knott colour rule and electrochemical analysis supported the explanation, with the HOMO energies of the equivalent dyes being the same with the LUMO energies of the ketocyanines being destabilised relative to the cyanines.

## 5. Acknowledgements

We thank EPSRC for financial support (Project number EP/E01075X/1). Professor Paul Burn is UQ Vice Chancellor's Senior Research Fellow. Seth Olsen acknowledges the support of the Australian Research Council through Discovery Project DP110101580 and the award of an Australian

Research Fellowship. We also acknowledge the University of Queensland for providing funding for Ross Jansen-van Vuuren (UQRS and UQIRA) and Brasenose College, University of Oxford for funding Peter Deakin (Senior Germaine Scholarship).

## Figures and Schemes

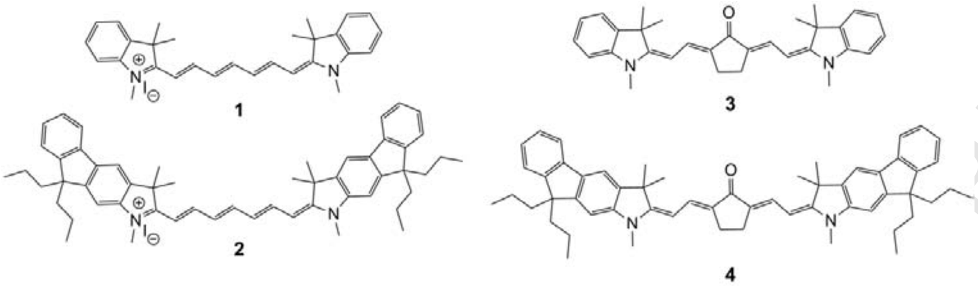

**Figure 1**. Chemical structures of cyanine **1**, fluorenylcyanine **2**, ketocyanine **3** and fluorenylketocyanine **4**.

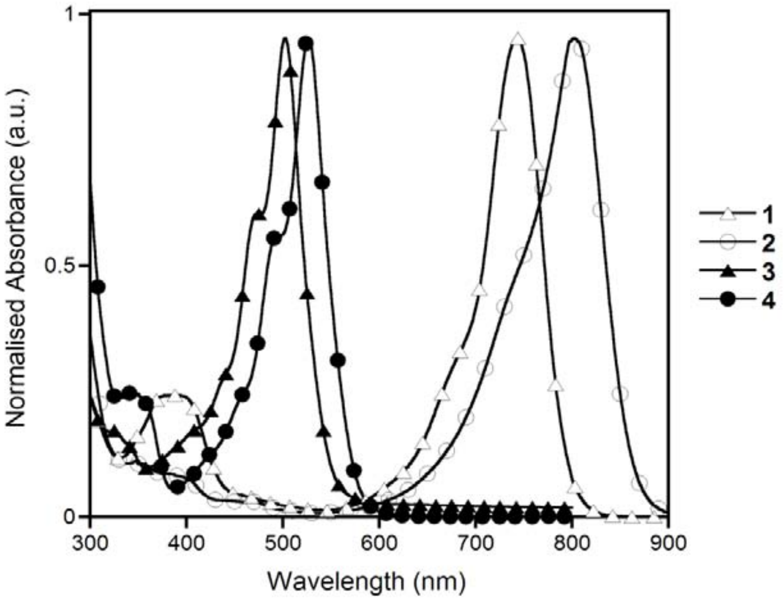

**Figure 2**. Normalised solution absorption spectra of **1**, **2**, **3** and **4** (in THF).

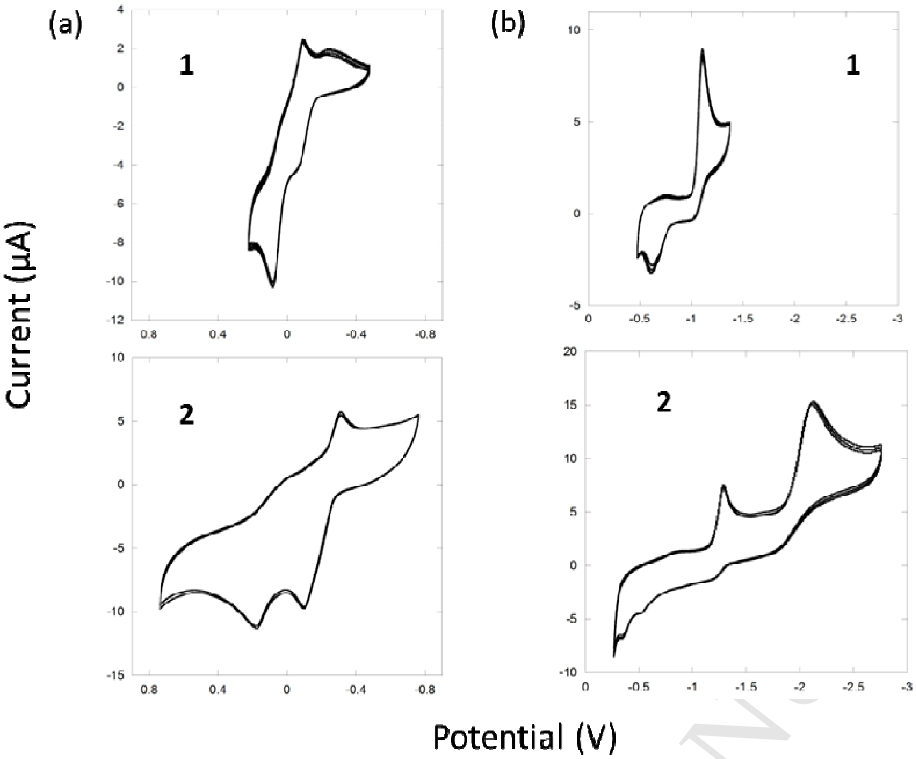

**Figure 3**. (a) Oxidation and (b) reduction cyclic voltammograms of **1** and **2**, obtained with scan rates of 100 mV/s (oxidation of **1** and **2**, and reduction of **2**) and 50 mV/s (oxidation of **2**).

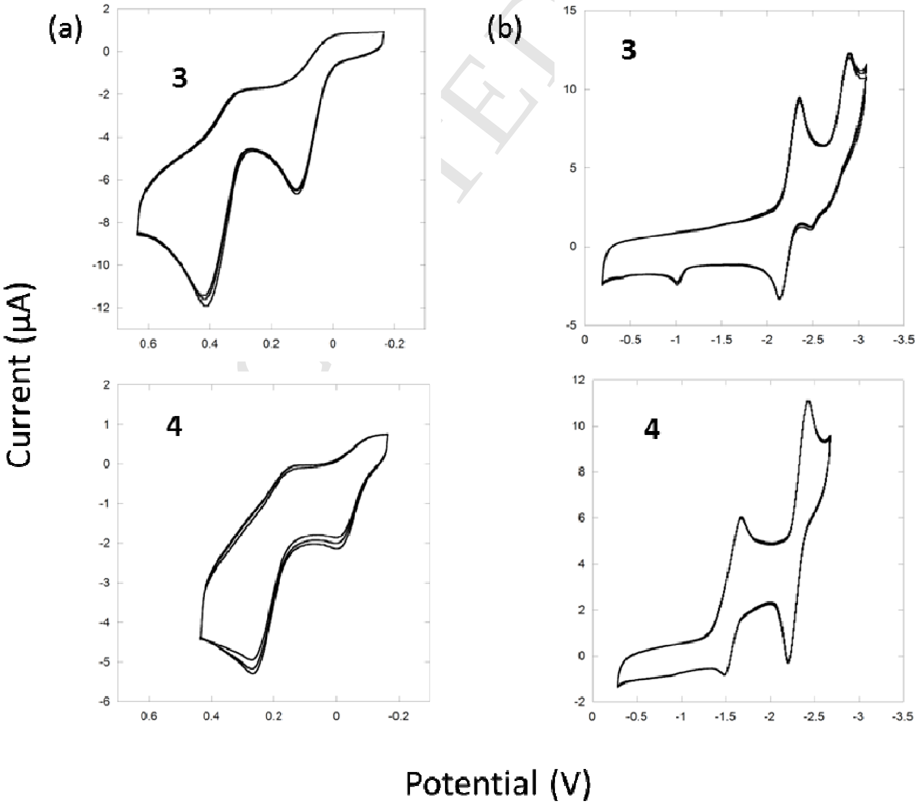

**Figure 4**. (a) Oxidation and (b) reduction cyclic voltammograms of **3** and **4**, obtained with scan rates of 100 mV/s (oxidation of **4** and reduction of **3** and **4**) and 200 mV/s (oxidation of **3**).

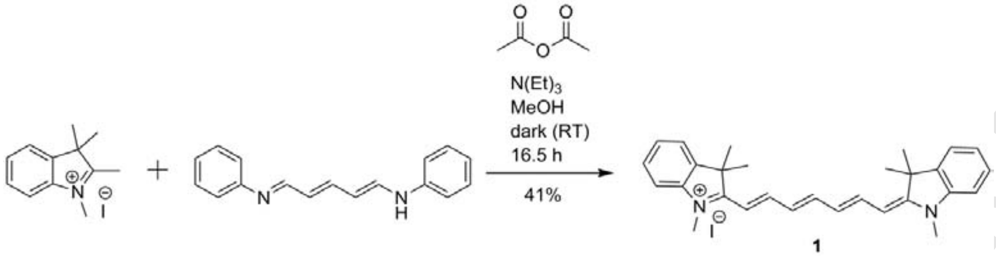

**Scheme 1.** Synthetic route to cyanine **1**.

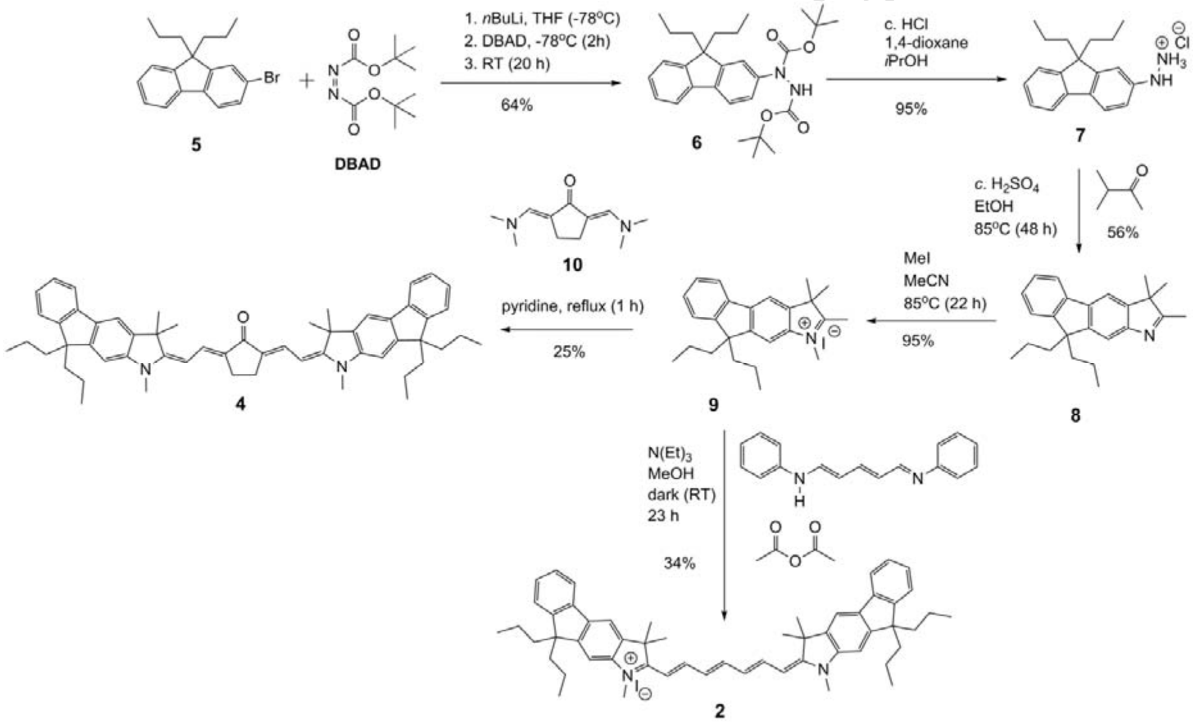

**Scheme 2.** Synthetic routes to fluorenylcyanine **2** and fluorenylketocyanine **4**.

## References

[1] Heeger, AJ. Semiconducting polymers: the Third Generation. Chem Soc Rev 2010; 39: 2354-2371.

[2] Brabec, CJ, Sariciftci, NS, Hummelen, JC. Plastic Solar Cells. Adv Funct Mater 2001; 11: 15-26.

[3] Yu G, Gao J, Hummelen, JC, Wudl F, Heeger AJ. Polymer Photovoltaic Cells: Enhanced Efficiencies via a Network of Internal Donor-Acceptor Heterojunctions. Science 1995; 270: 1789-1791.

[4] So F, Krummacher B, Mathai MK, Poplavskyy D, Choulis SA, Choong V-E. Recent progress in solution processable organic light emitting devices. J Appl Phys 2007; 102: 091101.

[5] Klauk H. Organic thin-film transistors. Chem Soc Rev 2010; 39: 2643-2666.

[6] Dimitrakopoulos CD, Malenfant PRL. Organic Thin Film Transistors for Large Area Electronics. Adv Mater 2002; 14: 99-117.

[7] Yu G, Wang J, McElvain J, Heeger AJ. Large-Area, Full-Color Image Sensors Made with Semiconducting Polymers. Adv Mater 1998; 10: 1431-1434.

[8] Wang J, Yu G, Srdanov G, Heeger AJ. Org Electron 2000; 1: 33-40.

[9] Gong X, Tong M, Xia Y, Cai W, Moon JS.; Cao Y, Yu G, Shieh C-L, Nilsson B, Heeger AJ. High-Detectivity Polymer Photodetectors with Spectral Response from 300 nm to 1450 nm. Science 2009; 325: 1665-1667.

[10] Fukuda T, Komoriya M, Kobayashi R, Ishimaru Y, Kamata N. Wavelength-Selectivity of Organic Photoconductive Devices by Solution Process. Jpn J Appl Phys 2009; 48: 04C162.

[11] Jansen-van Vuuren RD, Pivrikas A, Pandey AK, Burn PL. Colour selective organic photodetectors utilizing ketocyanine-cored dendrimers. J Mater Chem. C 2013; 1: 3532-3543.

[12] Yusuke H, Kyu-Sik K, Hyeon-Gu J, Musubu I. Enhancing spectral contrast in organic red-light photodetectors based on a light-absorbing and exciton-blocking layered system. J Appl Phys 2010; 108: 034502.

[13] Lupton JM, Koeppe R, Müller JG, Feldmann J, Scherf U, Lemmer U. Organic Microcavity Photodiodes. Adv Mater 2003; 15: 1471-1474.

[14] Silvestri F, Irwin MD, Beverina L, Facchetti A, Pagani GA, Marks TJ. Efficient Squaraine-Based Solution Processable Bulk-Heterojunction Solar Cells. J Amer Chem Soc 2008; 130: 17640-17641.

[15] Lin L-Y, Chen Y-H, Huang Z-Y, Lin H-W, Chou S-H, Lin F, Chen C-W, Liu Y-H, Wong K-T. A Low-Energy-Gap Organic Dye for High-Performance Small-Molecule Organic Solar Cells. J Amer Chem Soc 2011; 133: 15822-15825.

[16] Walker B, Kim C, Nguyen T-Q. Small Molecule Solution-Processed Bulk Heterojunction Solar Cells. Chem Mater 2010; 23: 470-482.

[17] Peumans, P, Yakimov A, Forrest SR. Small molecular weight organic thin-film photodetectors and solar cells. J Appl Phys 2003; 93: 3693-3723.

[18] Wu S-H, Li W-l, Chu B, Su Z-S, Zhang F, Lee CS. High performance small molecule photodetector with broad spectral response range from 200 to 900 nm. Appl Phys Lett 2011, 99, 023305.

[19] Castro FA, Benmansour H, Moser J-E, Graeff CFO, Nüesch F, Hany R. Photoinduced hole-transfer in semiconducting polymer/low-bandgap cyanine dye blends: evidence for unit charge separation quantum yield. Phys Chem Chem Phys 2009; 11: 8886-8894.

[20] Meng F, Chen K, Tian H, Zuppiroli L, Nüesch , F. Cyanine dye acting both as donor and acceptor in heterojunction photovoltaic devices. Appl Phys Lett 2003; 82: 3788-3790.

[21] Hany, R.; Fan, B.; de Castro, F. A.; Heier, J.; Kylberg, W.; Nüesch F. Strategies to improve cyanine dye multi layer organic solar cells. Prog Photovoltaics 2010; 19: 851-857.

[22] Fan B, Araujo de Castro F, Chu BT, Heier J, Opris D, Hany R, Nüesch F. Improved performance of cyanine solar cells with polyaniline anodes. J Mater Chem 2010; 20: 2952–2955.

[23] Izawa S, Hashimoto K, Tajima K. Efficient charge generation and collection in organic solar cells based on low band gap dyad molecules. Chem Commun 2011; 47: 6365-6367.

[24] Thompson BC, Fréchet JMJ. Polymer-Fullerene Composite Solar Cells. Angew Chem Int Edit 2008; 47: 58-77.

[25] Meng F, Hua J, Chen K, Tian H, Zuppiroli L, Nüesch F, Cyanine-fullerene dyad for application in broad spectral response photovoltaic devices. Proc of SPIE 2005; 5938: 593814.

[26] Bouit P, Rauh D, Neugebauer S, Delgado JL, Piazza ED, Rigaut S, Maury O, Andraud C, Dyakonov V, Martin N. A “Cyanine−Cyanine” Salt Exhibiting Photovoltaic Properties. Org Lett 2009; 11: 4806-4809.

[27] Chen P, Sun S, Hu Y, Qian Z, Zheng D. Structure and solvent effect on the photostability of indolenine cyanine dyes. Dyes Pigments 1999; 41: 227-231.

[28] Nüesch F, Faes A, Zuppiroli L, Meng F, Chen K, Tian H. Counterion effects in cyanine heterojunction photovoltaic devices. J Mater Sci 2005; 40: 1353-1357.

[29] Yu G, Gao J, Yang C, Heeger AJ. High-sensitivity photodetectors made with charge-transfer polymer blends. Proc of SPIE 1997; 2999: 306-314.

[30] Antognazza MR, Musitelli D, Perissinotto S, Lanzani G. Spectrally selected photodiodes for colorimetric application. Org Electron 2010; 11: 357-362.

[31] Lamprecht B, Thünauer R, Köstler S, Jakopic G, Leising G, Krenn JR. Spectrally selective organic photodiodes. Phys Status Solidi-R 2008; 2: 178-180.

[32] Jansen-van Vuuren RD, Johnstone KD, Ratnasingam S, Barcena H, Deakin PC, Pandey AK, Burn PL, Collins S, Samuel IDW. Determining the absorption tolerance of single chromophore photodiodes for machine vision. Appl Phys Lett 2010, 96: 253303.

[33] Mishra A, Behera RK, Behera PK, Mishra BK, Behera GB. Cyanines during the 1990s: A Review. Chem Rev 2000; 100: 1973-2012.

[34] Gritzner G, Kuta J. Recommendations on reporting electrode potentials in nonaqueous solvents: IUPC commission on electrochemistry. Electrochim Acta 1984; 29: 869-873.

[35] Jung JH, Lee KH, Yang CS. Synthesis and Physical Properties of Cyanine Dyes as Optical Information Recording Medium. J Korean Chem Soc 1998; 42: 570-574.

[36] Kawakami M, Kitaguchi H. Cyanine Dyes. US Patent 0054192 A1 2004; 26.

[37] Miltsov S, Encinas C, Alonso J. Novel synthesis of ketocyanine dyes. Tetrahedron Lett 2001; 42: 6129-6131.

[38] Robinson B. The Fischer Indole Synthesis. Chem Rev 1963; 63: 373-401.

[39] Wang, C.; Zhong, H.; Li, S.; Shu, W.; Shen, Y. Phenylacetylene Dendrimers Containing a Fluorene Core: Synthesis and Spectroscopic Studies. Chin J Chem 2010, 28, 699.

[40] Tatikolov AS, Krasnaya ZA, Shvedova LA, Kuzmin VA. Effects of chromophore interaction in photophysics and photochemistry of cyanine dyes. Int J Photoenergy 2000; 2: 23-.

[41] Brooker LGS. Absorption and Resonance in Dyes. Rev Mod Phys 1942; 14: 275-293.

[42] Platt JR. Wavelength Formulas and Configuration Interaction in Brooker Dyes and Chain Molecules. J Chem Phys 1956; 25: 80-105.

[43] Looney CW, Simpson WT. Structures and π-Electron Spectra. III. Triphenylmethane Dyes. J Amer Chem Soc 1954; 76: 6293-6300.

[44] Adam FC. The electronic spectra of diphenylmethane dyes. J Mol Spectrosc 1960; 4(1-6): 359-371.

[45] Dewar MJS. 478. Colour and constitution. Part I. Basic dyes. J Chem Soc (Resumed) 1950; 2329-2334.

[46] Knott EB. 227. The colour of organic compounds. Part I. A general colour rule. J Chem Soc (Resumed). 1951; 1024-1028.

[47] Olsen S. A quantitative quantum chemical model of the Dewar–Knott color rule for cationic diarylmethanes. Chem Phys Lett 2012; 532: 106-109.

[48] Spasokukotskii NS, Vompe AF. Color of cyanine dyes and polarizabilities of the groupings entering into the composition of the heterocyclic residues. J Appl Spectr 1970; 12: 81-84.

[49] Pandey AK, Deakin PC, Jansen-Van Vuuren RD, Burn PL, Samuel IDW. Photo-Rechargeable Battery Effect in First Generation Cationic-Cyanine Dendrimers Adv Mater 2010; 22: 3954-3958.

**Highlights**

- Cyanine and ketocyanine dyes containing 9,9-di-*n*-propylfluorenyl moieties are synthesized.
- The 9,9-di-*n*-propylfluorenyl units enable tuning of the optoelectronic properties of the dyes.
- The absorption properties of the dyes follow the Dewar-Knott colour rule.